Journal of Medicinal Chemistry

Article

pubs.acs.org/jmc

Radiofluorinated Derivatives of 2-(Phosphonomethyl)pentanedioic Acid as Inhibitors of Prostate Specific Membrane Antigen (PSMA) for the Imaging of Prostate Cancer

Keith Graham,* Ralf Lesche, Alexey V. Gromov, Niels Böhnke, Martina Schäfer, Jorma Hassfeld, Ludger Dinkelborg, and Georg Kettschau

Global Drug Discovery, Bayer HealthCare, Müllerstrasse 178, 13353, Berlin, Germany

ABSTRACT: For prostate cancer, prostate specific membrane antigen (PSMA) has been identified as a diagnostic and therapeutic target. Fluorinated derivatives of 2-(phosphonomethyl)pentanedioic acid were designed and synthesized to explore whether this fluorine-substituent is tolerated in the pentanedioic acid moiety that is common to almost all PSMA targeting small molecule inhibitors. The binding affinities of the racemic and individual stereoisomers of 2-fluoro-4-(phosphonomethyl)pentanedioic acid were determined and showed that the introduction of fluorine was well tolerated. The radiosynthesis of the analogous 2-[^{18}F]fluoro-4-(phosphonomethyl)pentanedioic acid was developed and evaluated in vivo with the PSMA positive LNCaP human prostate cancer cell. The biological results demonstrated specific binding of the tracer to PSMA positive tumors in mice. These results warrant the further evaluation of this class of compounds as radiolabeled tracers for the detection and staging of prostate cancer.

INTRODUCTION

Prostate cancer is the second leading cancer with more than 217 000 diagnosed cases in 2010 and is responsible for >30 000 prostate cancer-related deaths per year in the United States alone; only lung cancer has a higher mortality rate.[1] Prostate specific antigen (PSA), an in vitro diagnostic test, is currently used to screen for prostate cancer. However, this test has limited specificity and does not allow differentiation of localized from metastatic disease. Therefore, imaging procedures allowing specific detection of prostate cancer with high anatomic resolution would be highly desirable.

Currently, the only U.S. Food and Drug Administration approved radiopharmaceutical for imaging prostate cancer is ^{111}In-labeled capromab pendetide (ProstaScint, Cytogen). However, this antibody-based agent has had limited clinical use due to its slow distribution and clearance, which contributed to challenging image interpretation. Low molecular weight imaging agents for prostate cancer being pursued clinically include radiolabeled choline analogues,[6−10] *anti*-1-amino-3-[^{18}F]fluorocyclobutyl-1-carboxylic acid (*anti*-[^{18}F]F-FACBC),[11] [^{18}F]fluorodihydrotestosterone ([^{18}F]FDHT),[12] and 1-(2-deoxy-2-[^{18}F]fluoro-L-arabinofuranosyl)-5-methyluracil ([^{18}F]FMAU).[13] All of these agents have different uptake mechanisms, which can be advantageous like low urinary excretion for [^{11}C]choline and (*anti*[-^{18}F]F-FACBC), but most have various disadvantages, i.e., short physical half-life of the PET isotope (20 min for carbon-11 for [^{11}C]choline), high abdominal background for *anti*-[^{18}F]F-FACBC, or low-yielding multistep radiosynthesis for [^{18}F]FMAU.

One attractive target for primary and metastatic prostate cancer is the prostate specific membrane antigen (PSMA),[2−4] a type II integral membrane protein expressed in normal human prostate endothelium that is up-regulated in prostate cancer and its metastatic disease.[5] PSMA is also known as glutamate carbopeptidase II (GCPII) and folate hydrolase I (FOLH1) and exerts *N*-acetylate α-linked acidic dipeptidase (NAALADase) activity. Numerous different scaffolds are available for inhibiting PSMA and have been the topic of several recent reviews.[14,15] A number of these different PSMA scaffolds have been radiolabeled with SPECT and PET radioisotopes for the imaging of prostate cancer in the preclinical setting with promising results.[16−23] These scaffolds can be approximately split into three categories: (1) glutamate−urea heterodimers **1**;[16−20,23] (2) glutamate containing phosphoramidates **2**;[21] (3) 2-(phosphinylmethyl)pentanedioic acid **3**[22] (Figure 1).

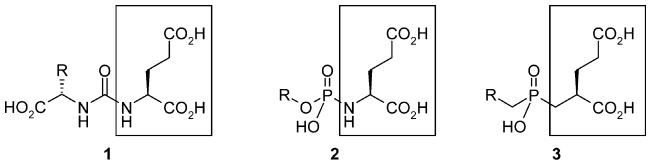

Figure 1. Structures of the PSMA scaffolds **1** (glutamate−urea heterodimer), **2** (glutamate phosphoramidate), and **3** (2-(phosphinylmethyl)pentanedioic acid), all containing a similar binding pentanedioic acid motif (dashed box).

The majority of published work focuses on the glutamate−urea heterodimer scaffold after the first promising results obtained with *N*-[*N*-[(*S*)-1,3-dicarboxypropyl]carbamoyl]-*S*-[^{11}C]methyl-L-cysteine ([^{11}C]DCMC) and *N*-[*N*-[(*S*)-1,3-dicarboxypropyl]carbamoyl]-*S*-3-[^{125}I]iodo-L-tyrosine ([^{125}I]-DCIT).[16] Presently the glutamate−urea−lysine heterodimer

Received: May 21, 2012

   dx.doi.org/10.1021/jm300710j | *J. Med. Chem.* XXXX, XXX, XXX−XXX

seems to be the heterodimer of choice, with subnanomolar binding affinity and impressive preclinical in vivo images being reported with various radioisotopes, i.e., fluorine-18,[19] gallium-68,[20] iodine-123,[18] iodine-131,[18] rhenium-188,[23] and technetium-99m.[23] Fluorine-18 is currently the isotope of choice, and selected examples that have shown promising preclinical results are illustrated in Figure 2, the glutamate–urea heterodimer scaffold (**4**[17] and **5**[19]) and the phosphoramidate scaffold (**6**[21]).

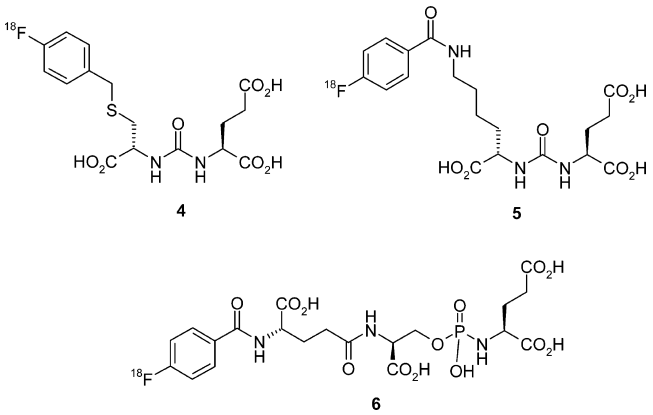

Figure 2. Known literature examples of the glutamate–urea–lysine heterodimer PSMA inhibitor scaffolds labeled with fluorine-18.

Structure–activity relationship studies on the glutamate or pentanedioic acid moiety show that any modification can be considerably detrimental to the binding affinity. The effect of stereochemistry at the 2-position shows that the *S*-isomer (2*S*)-**7** is 300-fold more affine than its *R*-isomer (2*R*)-**7** (Figure 3).[24] In addition, shortening or elongating the carbon chain between the two carboxylic acids results in a >500-fold loss in activity of **7** (0.3 nM) over **8** (700 nM) and **9** (185 nM).[25]

Efforts have been made by Kozikowski et al. to explore which substituents can be tolerated on the glutamate backbone. Unfortunately, simple substitutions with either a methyl or benzyl group in the 4-position of glutamate gave drastic losses in the affinity (Figure 4), surprisingly with methyl groups having a more pronounced effect in binding affinity (~150-fold decrease) than the bulkier benzyl groups (~50-fold decrease).[26]

Until recently it was assumed that the pentanedioic acid moiety within these binders could not be modified without considerable loss of affinity. However, Pomper et al. succeeded in identifying highly potent PSMA inhibitors featuring a modified glutamate portion featuring K_i values in the lower nanomolar range and thus being only moderately inferior with regard to 2-PMPA (0.3 nM). However, this was achieved starting from a picomolar inhibitor with intact glutamate portion (**20**, K_i = 0.01 nM, Figure 5), so the drop in activity was still considerable.[27]

Surprisingly, 2-PMPA (**7**), the first PSMA inhibitor discovered with subnanomolar activity and routinely used in vitro as the gold standard to determine the binding affinity of PSMA inhibitors, has not been investigated to see whether a radiolabeled derivative is useful for the imaging of prostate cancer. As fluorine-18 is the PET radioisotope of choice, with its 110 min half-life allowing the radiolabeled imaging agent to be produce centrally and distributed, we decided to investigate whether fluorinated derivatives of 2-PMPA would maintain their potency and when radiolabeled with fluorine-18, be suitable imaging agents for prostate cancer.

Herein, we report the synthesis, structure elucidation, and in vitro evaluation of the different stereoisomers of 2-fluoro-4-(phosphonomethyl)pentanedioic acid **21**. A suitable precursor **21** for direct labeling was synthesized to allow the radiofluorinated derivative [^{18}F]**21** to be synthesized in good yield and high radiochemical purity. This tracer was evaluated in vivo in mice bearing LNCaP tumor xenografts.

RESULTS AND DISCUSSION

Chemistry: Synthesis of the Fluorinated Reference Compounds. As outlined in Scheme 1, the key alcohol intermediate **22** was synthesized from methyl acrylate and methyl glyoxylate via an indium-mediated Barbier-type reaction in good yield (74%). This alcohol **22** was then subjected to a Vorbrüggen-type fluorination[28] employing nonafluorobutylsulfonyl fluoride and triethylamine tris-hydrofluoride to give the fluorinated derivative **23**. Subsequently, a phospho-Michael addition of dibenzylphosphite to the *α,β*-unsaturated ester **23** using potassium carbonate as a base led to the desired intermediate **24** in good yield. Diastereoselectivity in said Michael addition was low; typically, a ratio of approximately 1.5:1 was found in favor of the (2*R*,4*S*) and (2*S*,4*R*) isomers over (2*R*,4*R*) and (2*S*,4*S*), respectively. Acidic hydrolysis of all protecting groups was accomplished by heating in aqueous 6 M HCl to afford the mixture of different stereoisomers of **21**. Since we found **21** to be prone to spontaneous (re)-esterification in the presence of methanol, we performed the deprotection in two cycles, with intermediate evaporation of all volatiles and renewed exposure to 6 M HCl, in order to accomplish truly complete deprotection.

As a result of the pronounced polarity of **21**, we found ourselves unsuccessful in separating its stereoisomers by means of chiral HPLC even when screening a significant variety of stationary phases (data not shown). Therefore, the individual stereoisomers of **24** were prepared via two subsequent isomer separations using preparative chiral HPLC methods after the Vorbrüggen fluorination and after the phospho-Michael addition, respectively, to give the desired stereoisomers (2*R*,4*R*)-**24**, (2*R*,4*S*)-**24**, (2*S*,4*R*)-**24**, and (2*S*,4*S*)-**24** (Scheme 2). Most gratifyingly, the basic conditions of the phospho-Michael addition did not at all compromise the stereochemical integrity at the stereocenter just established in (*S*)-**23** and (*R*)-

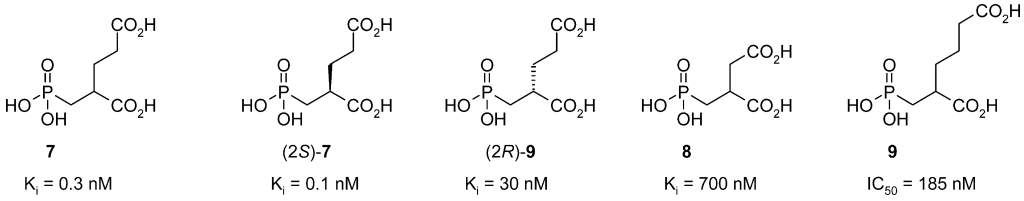

Figure 3. Effect of stereochemistry and chain elongation of the PMPA scaffold.

dx.doi.org/10.1021/jm300710j | J. Med. Chem. XXXX, XXX, XXX–XXX

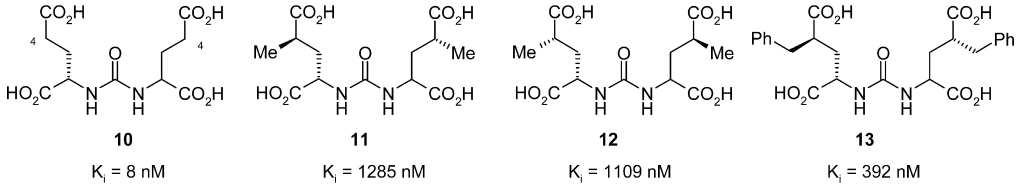

Figure 4. Effects of substitution on the glutamate backbone.

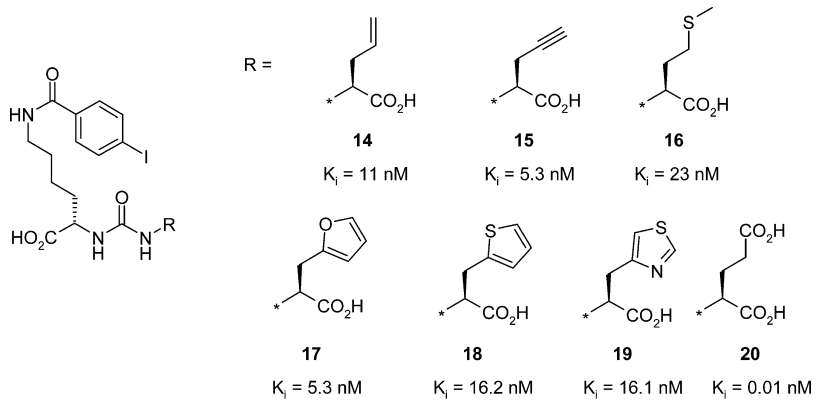

Figure 5. Substitution successfully tolerated in the P1′ site.

Scheme 1. Synthesis of Racemic Fluorinated PMPA Derivative 21[a]

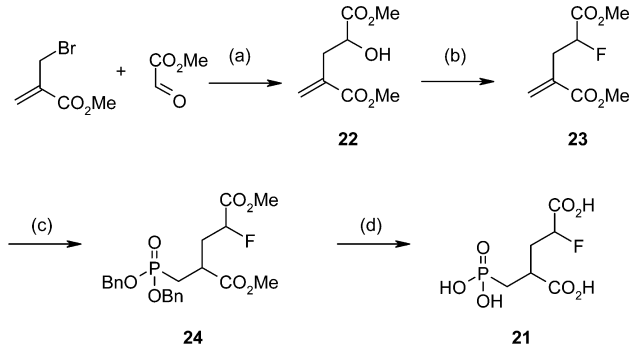

[a](a) In, MeOH, 0.3 M HCl aq, 4 h, rt, 74%; (b) $C_4F_9SO_2F$, $Et_3N{\cdot}3HF$, Et_3N, THF, 20 h, rt, 72%; (c) $(BnO)_2P(O)$, K_2CO_3, DMF, 4 h, 50 °C, 84%; (d) 6 M HCl aq, 60 °C, 30 h, 50%.

23. Again, deprotection of the stereoisomers of **24** was accomplished by acidic hydrolysis in 6 M aqueous hydrochloric acid. With regard to chemical naming it is noteworthy that the atom numbering of the pentadioic acid backbone reverts from **24** to **21** as a result of protecting group removal.

The respective absolute stereochemistry of the different isomers was assigned by X-ray crystallography of (2*R*,4*R*)-**21** (Figure 8), in combination with assignments based on their enantiomeric and diastereomeric relationship with each other, which is evident from the NMR spectra (enantiomers give identical NMR spectra, while different NMR spectra indicate diastereomeric relationship), but also from their respective chiral pHPLC separation history. Said assignments of absolute stereochemistry were further corroborated by additional X-ray analyses data of (2*S*,4*S*)-**25** (Figure 9) which was formed from (2*S*,4*S*)-**24** by catalytic hydrogenolysis (Scheme 3).[29]

Chemistry: Synthesis of the Radiolabeling Precursor. For the radiolabeling and in vivo experiments described below, precursor **28** was prepared by silylation of alcohol **22**, followed by phospho-Michael addition to give intermediate **27**. Silyl ether cleavage with excess HF·pyridine complex proceeded smoothly to give the intermediate γ-hydroxy ester which was immediately reacted with tosyl anhydride in pyridine to give tosylate **28** in good yield without substantial formation of the corresponding lactone. Not surprisingly, desilylation of **27** with TBAF instead of HF·pyridine resulted in fast and complete formation of the corresponding lactone (data not shown).

However, the need to employ large excesses of highly toxic HF·pyridine complex and the intermediacy of a highly lactonization prone γ-hydroxy ester warranted scouting for a more practical route, in particular for scaling purposes. Thus, key intermediate **22** was reacted with *p*-toluenesulfonic anhydride to give the intermediate **29**. When investigating the phospho-Michael addition to **29**, we were fairly concerned that the leaving group qualities of the tosylate could result in elimination to give a fully conjugated unsaturated diester. When investigating the reaction with a broad range of bases, we surprisingly found DBU, actually well-known as a reagent to induce elimination, to be by far the most suitable base for this reaction to afford the desired product **28** in good yield as outlined in Scheme 4.

Radiochemistry. To establish a suitable radiosynthesis method, precursor **28** was used as a mixture of stereoisomers. The first step was the nucleophilic displacement of the tosylate group in the 4-position with [^{18}F]fluoride. The noncarrier added (nca) nucleophilic fluorination of precursor **28** was accomplished in DMSO at 120 °C in the presence of cesium carbonate and Kryptofix 2.2.2. as a phase transfer catalyst (PTC), and the intermediate [^{18}F]**24** was purified using semipreparative HPLC methods, as we envisioned difficulties in purifying the final radiolabeling product away from similar polar byproducts that could interfere with any subsequent biological testing. The purified [^{18}F]-labeled intermediate [^{18}F]**24** was subjected to a strongly acidic deprotection step using 6 M hydrochloric acid at 120 °C to remove the two methylcarboxylic esters and the two benzylic phosphonate esters. The resulting strongly acidic reaction mixture was then passed

dx.doi.org/10.1021/jm300710j | J. Med. Chem. XXXX, XXX, XXX−XXX

Scheme 2. Synthesis of the Different Stereoisomers of 21[a]

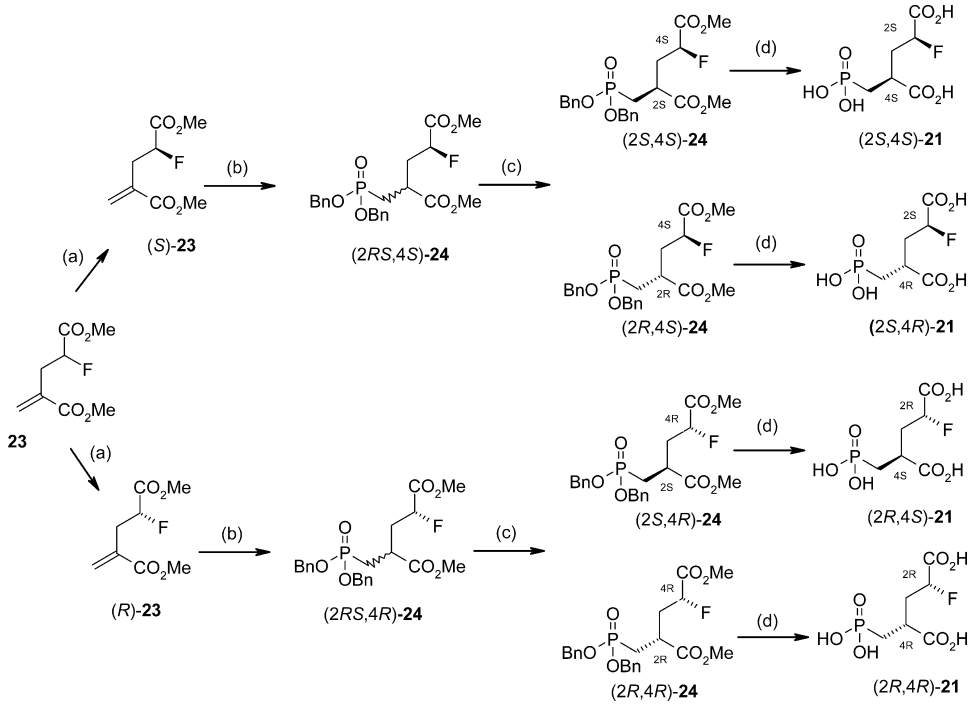

[a](a) Chiral preparative HPLC (Chiralpak IC); (b) $(BnO)_2P(O)H$, K_2CO_3, DMF, 50 °C, 2 h, 96/98% yield; (c) chiral preparative HPLC (Chiralcel OD-H); (d) 6 M HCl aq, 50 °C, 30 h, 80% range.

Scheme 3. Synthesis of the Derivative (2*S*,4*S*)-25 for X-ray Crystallography[a]

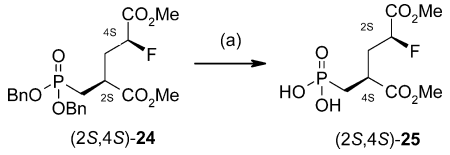

[a](a) Pd/C, H_2, THF, 2 h, rt, 70%.

Scheme 5. Synthesis of the Radiolabeled Racemic [^{18}F]21[a]

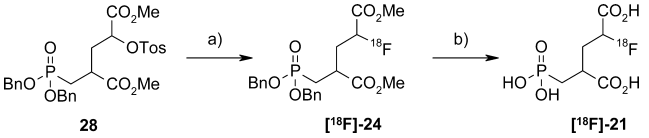

[a](a) K[^{18}F]F, K_{222}, DMSO, 120 °C, 15 min; (b) 6 M HCl aq, 120 °C, 15 min.

through an AG-11A8 resin and a C18 solid phase extraction cartridge (SPE) and washed with saline to give the desired product [^{18}F]**21** (Scheme 5) as a formulated solution ready for biological testing. The identity of [^{18}F]**21** was confirmed by co-injection of the corresponding cold reference, using a Corona aerosol detector (CAD) connected to the HPLC instrument (Figure 6), as this detector is known to detect non-UV polar

Scheme 4. Syntheses of the Precursor 28 (Optimized Route, as Mixture of Stereoisomers)[a]

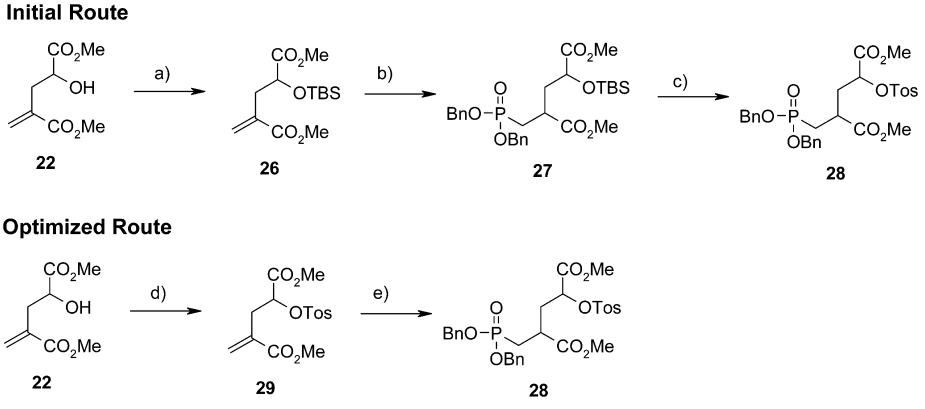

[a]Initial route: (a) TBSCl, *N*-Me-imidazole, CH_2Cl_2, 0 °C then 16 h rt, 84%; (b) $(BnO)_2P(O)H$, K_2CO_3, DMF, 2 h 90 °C then 60 h rt, 98%; (c) (i) HF·py 50 equiv, THF, 4 h rt, (ii) Tos_2O, pyridine, 16 h rt, 70% overall. Optimized route: (d) Tos_2O, pyridine, 2 h at 0 °C, then 16 h rt, 99%; (e) $(BnO)_2P(O)H$, DBU, THF, 1.5 h rt, 61%.

dx.doi.org/10.1021/jm300710j | J. Med. Chem. XXXX, XXX, XXX−XXX

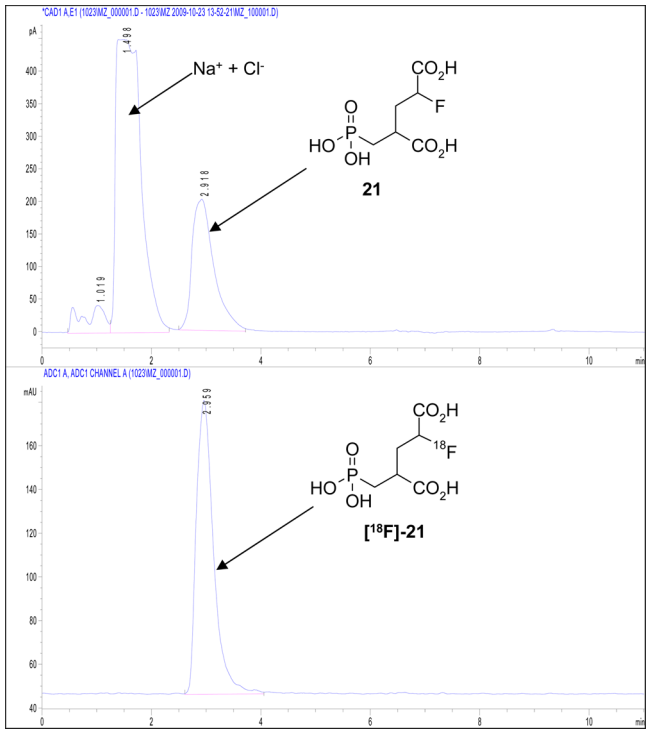

Figure 6. HPLC analysis of the final product [^{18}F]**21** with co-injection of the reference standard **21** (top chromatogram with Corona detector, bottom chromatogram with γ detector).

compounds with a high degree of sensitivity (detection limit using this method was determined to be 1 μg/mL, and the specific activity of the tracer was always below the limit of detection and calculated to be >25GBq/μmol). The final product was analyzed by TLC, and the radiochemical was found to be >95% with about 3−4% free [^{18}F]fluoride[30,31]

Biological Characterization. *In Vitro Binding.* In vitro potency of PSMA inhibitors was determined by inhibiting NAALADase, one of the enzymatic activities reported for PSMA.[32] NAALADase activity was determined in membrane lysates from LNCaP cells, reported to express high amounts of PSMA.[33] NAALADase inhibition was determined by measuring the release of [^{3}H]glutamate from the PSMA substrate [^{3}H]NAAG in the presence of increasing concentrations of inhibitor and resulted in K_i values of 0.4 ± 0.2 nM and 2.6 ± 0.4 nM for 2-PMPA and racemic **21**, respectively. Among the four stereoisomers compounds, (2*S*,4*S*)-**21** and (2*R*,4*S*)-**21** showed significantly higher potency to inhibit NAALADase activity compared to (2*S*,4*R*)-**21** and (2*R*,4*R*)-**21**, respectively (see Table 1 for details). The next natural step was to carry out in vivo experiments; it was decided to investigate the radiolabeled racemic derivative [^{18}F]**21** to determine whether this scaffold showed promise for imaging PSMA expression in PSMA positive tumor bearing xenographs. Positive visualization of the tumor would then warrant further investigations into the different radiolabeled stereoisomers of [^{18}F]**21**, as new analytical methods would need to be developed to analyze the final product for stereochemistry integrity.

Table 1. NAALADase Inhibition of Fluorinated PMPA Compounds

compd	IC_{50} (nM)	K_i (nM)
21	6.8 ± 0.7	2.6 ± 0.4
(2*S*,4*S*)-**21**	3.1 ± 0.8	1.4 ± 0.6
(2*R*,4*S*)-**21**	8.1 ± 0.7	3.1 ± 0.3
(2*S*,4*R*)-**21**	55.9 ± 3.1	22.0 ± 1.1
(2*R*,4*R*)-**21**	89.4 ± 13.2	36.4 ± 6.3
7	1.1 ± 0.6	0.4 ± 0.2

Micro-PET/CT Imaging. Racemic [^{18}F]**21** was injected into nude mice bearing LNCaP tumors. Images of different animals were recorded at 45−75 min and 110−130 min after injection, respectively (shown in Figure 7). Racemic [^{18}F]**21** allowed clear tumor visualization at both time points, whereas uptake into other organs was observed mainly in bladder, kidney, and to a lesser degree, bone. No visualization of liver and gut and continuous accumulation of the tracer into the bladder pointed to renal elimination as the predominant excretion pathway. Since bone uptake did not increase over time, we found no evidence for compound disintegration caused by accumulation of free fluoride. Instead, residual free fluoride from the radiopreparation (3−4% estimated by TLC) contributed to the observed bone accumulation. Preinjection of unlabeled **21** resulted in significant decrease of signal from the tumor, confirming specific binding of [^{18}F]**21** to LNCaP tumors. Interestingly, tracer accumulation in kidney was also reduced upon blocking with **21**, pointing to specific binding of the tracer. This observation is in line with previous reports of high PSMA expression in proximal tubules of rodent kidneys[34,35] and comparable to high and specific binding to kidney reported for other radiotracers targeting PSMA.[20,21]

CONCLUSIONS

The syntheses of different fluorinated stereoisomeric derivatives of PMPA (the in vitro gold standard) showed that fluorine was surprisingly well tolerated in the pentanedioic acid binding portion, despite previous reports showing that small substitutions in this portion resulted in >100-fold loss in binding affinity.[25,26] Two of the four stereoisomers, (2*R*,4*S*)-**21** (K_i = 3.1 nM) and (2*S*,4*S*)-**21** (K_i = 1.4 nM), were identified to be highly potent inhibitors of PSMA. [^{18}F]-Labeled **21** was synthesized as a mixture of stereoisomers and showed promising images in LNCaP tumor bearing mice. These results warrant the further evaluation of the different stereoisomers of [^{18}F]-**21** in vivo.

EXPERIMENTAL SECTION

General. Chemicals and solvents were used as received from commercial vendors Sigma Aldrich (Taufkirchen, Germany), Tocris Bioscience (Bristol, U.K.), Alexis Biochemical (now Enzo Life Sciences, Loerrach, Germany), Bachem AG (Bubendorf Switzerland), Toronto Research Chemicals Inc. (North York, Ontario, Canada), and Acros Organics (part of Thermo Fisher-Scientific, Nidderau, Germany). Monomeric methyl glyoxylate was purchased from Waterstone, Inc., Carmel, IN, U.S. [^{18}F]Fluoride was produced via an ^{18}O(p,n)^{18}F nuclear reaction and was supplied by EuroPET (Berlin, Germany). Chemical reactions were monitored by TLC and by UPLC/MS analysis of reaction mixtures (Waters Aqcuity with single quadrupole ESI-MS detector). Crude products were, unless stated otherwise, purified on silica gel (KP-SIL cartridges, Biotage) on automated flash cromatography devices (SP-4 or Isolera Four by Biotage). Stereoisomer separations were performed by chiral HPLC according to the methods specified below. ^{1}H and ^{19}F nuclear magnetic resonance (NMR) spectra were recorded with Bruker AVANCE 300 and 400 MHz and the Bruker DRX-600 NMR spectrometers. Chemical shifts (δ) are expressed in parts per million relative to tetramethylsilane. Coupling constants (J) are expressed in hertz (Hz), and the following abbreviations are used to describe the

dx.doi.org/10.1021/jm300710j | J. Med. Chem. XXXX, XXX, XXX−XXX

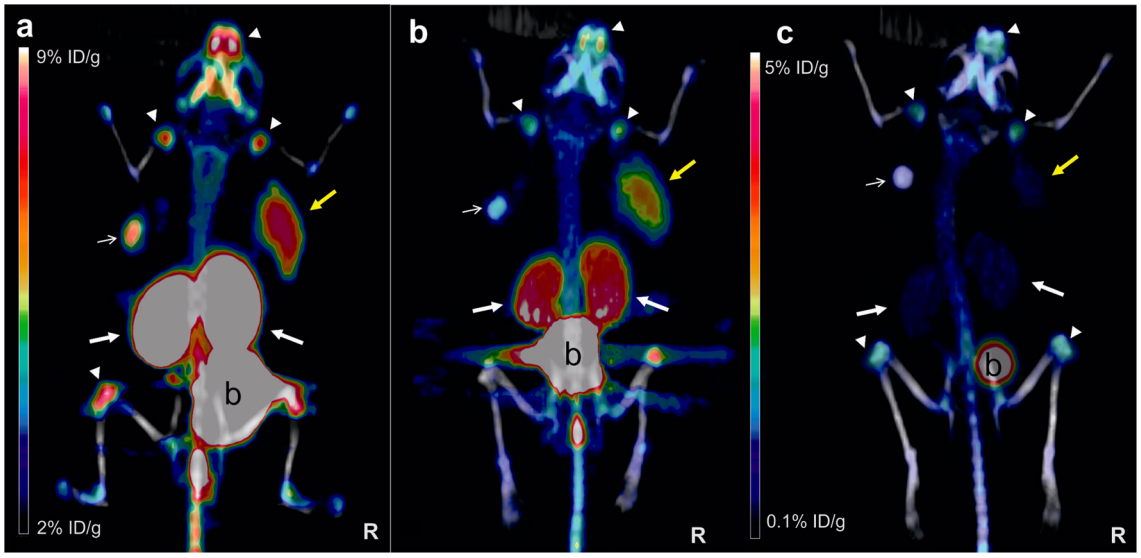

Figure 7. PET/CT imaging of [^{18}F]**21**. Human LNCaP prostate tumor-bearing mice were used for tumor visualization by PET. Whole body PET data (in rainbow colors) were acquired and fused with the CT image (in gray). Strong tumor signals (yellow arrow) were found 45−75 min pi (a) and 110−130 min (b). Tumor uptake was significantly reduced by preinjection of excess cold reference **21** (110−130 min pi) (c), confirming specific binding of [^{18}F]**21** to LNCaP tumors. The high background signals observed in bladder (b) were due to excretion. Besides renal excretion the strong signals in kidneys (filled arrows) were caused by specific binding of the tracer to PSMA which is expressed in rodent kidney.[34,35] Bone uptake (arrow heads point to skull and joints) did not increase over time and was primarily due to residual [^{18}F]fluoride in the radiopreparation. Open arrows point to testosterone pellets that were implanted to stimulate growth of the androgen dependent LNCaP tumor cells.

appearance of peak patterns: s (singlet), d (doublet), t (triplet), q (quartet), quint (quintet), combinations thereof (e.g., dd, doublet of doublet), m (multiplet), mc (centered multiplet), and br (broad signal). Purity all compounds including **21** and its stereoisomers was judged to be in the 95% range according to H NMR, with no chemical impurity detectable. For the isomeric mixture and the active stereoisomers, this was confirmed by F NMR vs fulvestrant as internal standard; yields were adjusted accordingly. Chiral HPLC methods were carried out using the following analytical and preparative methods. Analytical method 1 consisted of the following: Chiralpak IC 5 μm column (150 mm × 4.6 mm) with a flow rate of 1.0 mL/min at 25 °C using UV detection at 210 nm. The solvent system used was isocratic (hexane/2-propanol, 80:20). Analytical method 2 consisted of the following: Chiralcel OD-H 5 μm column (150 mm × 4.6 mm) with a flow rate of 1.0 mL/min at 25 °C using UV detection at 210 nm. The solvent system used was isocratic (hexane/ethanol, 85:15). Preparative method 1 consisted of the following: Chiralpak IC 5 μm column (250 mm × 30 mm) with a flow rate of 40.0 mL/min at ambient temperature using UV detection at 210 nm. The solvent system used was isocratic (hexane/2-propanol, 80:20). Preparative method 2 consisted of the following: Chiralcel OD-H 5 μm column (250 mm × 20 mm) with a flow rate of 20.0 mL/min at ambient temperature using UV detection at 210 nm. The solvent system used was isocratic (hexane/ethanol, 85:15). X-ray crystallography analyses were performed at 100 K on either a Bruker X8 Proteum Microstar diffractometer with Helios Cu X-ray optics ((2*S*,4*S*)-**25**) or a Bruker SMART platform diffractometer with Osmic Cu X-ray optics (Cu Kα, λ = 1.541 78 Å) ((2*R*,4*R*)-**21**), respectively. The single crystals were mounted on a cryoloop using a protective oil. X-ray data collection and processing of data were performed using the PROTEUM2 program.[36] Absorption correction was performed using SADABS.[37] SHELXS was used for structure solution, and SHELXL was used for full matrix least-squares refinement on F^2.[37] All non-hydrogen atoms were refined anisotropically. All H atoms were added in calculated positions and refined riding on their resident atoms. The stereochemistry could be assigned unambiguously. The program XP in the SHELXTL package was used for molecular representations.[37] Radioanalytical HPLC runs were performed on an Agilent 1100, and preparative HPLC runs were performed on a Knauer Smartline 1000. Purification was done on a semipreparative ACE RP C18 column (10 mm × 250 mm, 5 μm; Advanced Chromatographic Technologie). The elution solution was 60% acetonitrile/40% water with 0.1% trifluoroacetic acid at a flow of 4 mL/min. Radiochemical purity was analyzed on a ZIC HILIC column (4.6 mm × 100 mm, 5 μm; SeQuant), and radioactivity detection was performed on a GABI Star from Raytest. The elution solution was 0.1 M ammonium formate (pH 3.2)/actonitrile (3:7), and the flow rate was 0.5 mL/min. The non-UV active cold reference compound was detected on a Corona charged aerosol detector (CAD) from ESA.The tumor cell lines were obtained from ATTC (U.S.) or DSZM (Germany) if not otherwise indicated and maintained according to protocols provided by the supplier.

Dimethyl 2-Hydroxy-4-methylenepentanedioate (22). In a three-necked flask equipped with a powerful mechanical stirrer, to a cooled (+5 °C, ice−water bath) mixture of methyl glyoxylate (10.0 g, 114 mmol), methyl (2-bromomethyl)acrylate (22.5 g, 1.10 equiv), methanol (80 mL), and 0.3 N aqueous hydrochloric acid (80 mL) was added powdered indium (100 mesh, 13.0 g, 1.00 equiv) in several portions, maintaining the internal temperature below 35 °C (which did not require full cooling during the addition of the later portions). The cooling bath was then completely removed. Several freshly broken glass shards (from a Pasteur pipet, to scratch clotting pieces of the indium) were added, and the mixture was stirred vigorously for 4 h, during which the mixture cooled to room temperature. The mixture was decanted from all solids, and the supernatant was concentrated in vacuo. The residue was saturated with solid sodium chloride and then extracted with MTBE. The residue remaining hereafter was loaded on Celite and was washed with MTBE (4×) and EtOAc (1×). The combined organic layers were dried over sodium sulfate, passed over a plug of Celite, and evaporated. The residue was purified by column chromatography over silica to give 16.8 g of the target compound in 94% purity (74% yield): ^{1}H NMR (300 MHz, $CDCl_3$) δ ppm 2.65 (dd, 1 H), 2.87 (dd, 1 H), 3.07 (s br, 1 H), 3.77 (s, 3 H), 3.78 (s, 3 H), 4.34−4.44 (m, 1 H), 5.74 (m, 1 H), 6.30 (m, 1 H). MS (CI): $[M + H]^+$ = 189. MS (CI): $[M + NH_4]^+$ = 206.

Dimethyl 2-Fluoro-4-methylenepentanedioate (23). To a solution of **22** (6.00 g, 31.9 mmol) in THF (60 mL) were added at room temperature perfluorobutanesulfonic acid fluoride (11.7 mL, 2.00 equiv), triethylamine trihydrofluoride (10.4 mL, 2.00 equiv), and triethylamine (26.7 mL, 6.00 equiv). After being stirred for 20 h at room temperature, the reaction mixture was partitioned between water

dx.doi.org/10.1021/jm300710j | J. Med. Chem. XXXX, XXX, XXX−XXX

and dichloromethane. The organic layer was separated and washed with a brine/water mixture (1:1), dried over sodium sulfate, and concentrated under reduced pressure. The crude product was purified by column chromatography (silica, hexane/EtOAc) to give the desired fluoride (4.37 g, 72% yield): ^{1}H NMR (400 MHz, $CDCl_3$) δ ppm 2.76−2.88 (m, 1 H), 2.94−3.06 (m, 1 H), 3.79 (s, 3 H), 3.80 (s, 3 H), 5.18 (ddd, 1 H), 5.78 (s, 1 H), 6.35 (s, 1 H). MS (ESI): $[M + H]^+$ = 191.

Dimethyl (*S*)-2-Fluoro-4-methylenepentanedioate ((*S*)-23). (*S*)-**23** was obtained from racemic **23** by means of preparative chiral HPLC (preparative method 1): t_R = 4.8 min (chiral HPLC, analytical method 1).

Dimethyl (*R*)-2-Fluoro-4-methylenepentanedioate ((*R*)-23). (*R*)-**23** was obtained from racemic **23** by means of preparative chiral HPLC (preparative method 1): t_R = 6.3 min (chiral HPLC, analytical method 1).

Dimethyl *rac*-2-{[Bis(benzyloxy)phosphoryl]methyl}-4-fluoropentanedioate (24). To a solution of **23** (50 mg, 0.26 mmol) and dibenzyl phosphite (86 mg, 1.25 equiv) in DMF (3 mL) was added finely powdered potassium carbonate (mesh 325, 55 mg, 1.50 equiv), and the resulting mixture was heated to 50 °C for 4 h in a microwave oven. After cooling to room temperature, the mixture was partitioned between EtOAc and 5% aqueous citric acid. The organic layer was washed with half-concentrated brine, dried over sodium sulfate, and evaporated. The residue was purified by column chromatography over silica gel (hexane/EtOAc) to give the target compound as a mixture of stereoisomers (99 mg, 84% yield): ^{1}H NMR (400 MHz, $CDCl_3$) δ ppm 1.88−2.04 (m, 1 H), 2.10−2.39 (m, 3 H), 2.91−3.08 (m, 1 H), 3.55 (s, 3 H, minor diastereomer), 3.58 (s, 3 H, major diastereomer), 3.76 (s, 3 H, minor diastereomer), 3.77 (s, 3 H, major diastereomer), 4.82−5.08 (m, 5 H), 7.29−7.41 (m, 10 H). MS (ESI): $[M + H]^+$ = 453. The reaction was also performed on an 80 g scale under somewhat modified conditions (DBU, 1.25 equiv (instead of K_2CO_3), dibenzyl phosphite (2.0 equiv) in THF, 3 h room temperature, 46%).

Dimethyl (2*S*,4*S*)-2-{[Bis(benzyloxy)phosphoryl]methyl}-4-fluoropentanedioate ((2*S*,4*S*)-24) and Dimethyl (2*R*,4*S*)-2-{[Bis(benzyloxy)phosphoryl]methyl}-4-fluoropentanedioate ((2*R*,4*S*)-24). To a solution of (*S*)-**23** (500 mg, 2.39 mmol, 91% purity) in DMF (4.0 mL) was added finely powdered potassium carbonate (325 mesh, 595 mg, 1.80 equiv) and dibenzyl phosphite (1.00 g, 1.60 equiv), and the resulting mixture was stirred at 50 °C for 2 h in a microwave oven. After cooling to room temperature, the mixture was partitioned between EtOAc and 5% aqueous citric acid, and the organic layer was washed with brine, dried over sodium sulfate, and evaporated. Column chromatography over silica gel (hexane/EtOAc) gave 1.04 g (96% yield) of the target compound as a mixture of the two (4*S*) epimers, which was separated by means of chiral HPLC (preparative method 2) to give (2*S*,4*S*)-**24** (340 mg, 31% yield) and (2*R*,4*S*)-**24** (470 mg, 43% yield).

Dimethyl (2*S*,4*S*)-2-{[Bis(benzyloxy)phosphoryl]methyl}-4-fluoropentanedioate ((2*S*,4*S*)-24). t_R = 10.7 min (chiral HPLC, analytical method 2); ^{1}H NMR (300 MHz, $CDCl_3$) δ ppm 1.90−2.06 (m, 1 H), 2.11−2.39 (m, 3 H), 2.89−3.06 (m, 1 H), 3.55 (s, 3 H), 3.76 (s, 3 H), 4.82−5.11 (m, 5 H), 7.27−7.43 (m, 10 H).

Dimethyl (2*R*,4*S*)-2-{[Bis(benzyloxy)phosphoryl]methyl}-4-fluoropentanedioate ((2*R*,4*S*)-24). t_R = 7.1 min (chiral HPLC, analytical method 2); ^{1}H NMR (300 MHz, $CDCl_3$) δ ppm 1.86−2.02 (m, 1 H), 2.09−2.42 (m, 3 H), 2.93−3.10 (m, 1 H), 3.58 (s, 3 H), 3.77 (s, 3 H), 4.79−5.11 (m, 5 H), 7.27−7.44 (m, 10 H). The preparation was adapted to larger scale starting from (*S*)-**23** (2.75 g) being reacted with 1.40 equiv of dibenzyl phosphite and 1.60 equiv of potassium carbonate under otherwise unchanged conditions to give (2*S*,4*S*)-**24** (2.02 g) and (2*R*,4*S*)-**24** (3.03 g).

Dimethyl (2*S*,4*R*)-2-{[Bis(benzyloxy)phosphoryl]methyl}-4-fluoropentanedioate ((2*S*,4*R*)-24) and Dimethyl (2*R*,4*R*)-2-{[Bis(benzyloxy)phosphoryl]methyl}-4-fluoropentanedioate ((2*R*,4*R*)-24). To a solution of (*R*)-**23** (500 mg, 2.39 mmol, 91% purity) in DMF (4.0 mL) were added finely powdered potassium carbonate (325 mesh, 595 mg, 1.80 equiv) and dibenzyl phosphite (1.00 g, 1.60 equiv), and the resulting mixture was stirred at 50 °C for 2 h in a microwave oven. After cooling to room temperature, the mixture was partitioned between EtOAc and 5% aqueous citric acid, and the organic layer was washed with brine, dried over sodium sulfate, and evaporated. Column chromatography over silica gel (hexane/EtOAc) gave 1.06 g (98% yield) of the target compound as a mixture of the two (4*R*) epimers, which were separated by means of chiral HPLC (preparative method 2) to give (2*S*,4*R*)-**24** (480 mg, 44% yield) and (2*R*,4*R*)-**24** (340 mg, 31% yield).

Dimethyl (2*S*,4*R*)-2-{[Bis(benzyloxy)phosphoryl]methyl}-4-fluoropentanedioate ((2*S*,4*R*)-24). t_R (chiral HPLC, analytical method 2) = 8.8 min; ^{1}H NMR (300 MHz, $CDCl_3$) δ ppm 1.86−2.02 (m, 1 H), 2.09−2.42 (m, 3 H), 2.93−3.10 (m, 1 H), 3.58 (s, 3 H), 3.77 (s, 3 H), 4.79−5.11 (m, 5 H), 7.27−7.44 (m, 10 H).

Dimethyl (2*R*,4*R*)-2-{[Bis(benzyloxy)phosphoryl]methyl}-4-fluoropentanedioate ((2*R*,4*R*)-24). t_R (chiral HPLC, analytical method 2) = 9.4 min; ^{1}H NMR (300 MHz, $CDCl_3$) δ ppm 1.90−2.06 (m, 1 H), 2.11−2.39 (m, 3 H), 2.89−3.06 (m, 1 H), 3.55 (s, 3 H), 3.76 (s, 3 H), 4.82−5.11 (m, 5 H), 7.27−7.43 (m, 10 H). The preparation was adapted to larger scale starting from (*R*)-**23** (2.58 g) being reacted with 1.40 equiv of dibenzyl phosphite and 1.60 equiv of potassium carbonate under otherwise unchanged conditions to give (2*S*,4*R*)-**24** (2.28 g) and (2*R*,4*R*)-**24** (1.49 g).

***rac*-2-Fluoro-4-(phosphonomethyl)pentanedioic Acid (21).** A mixture of **24** (34 g, 75 mmol) in aqueous 6 N hydrochloric acid (340 mL) was stirred for 6 h at 60 °C. The mixture was then evaporated (to remove methanol formed during hydrolysis). Again, 6 M hydrochloric acid (340 mL) was added, and the mixture was stirred at 60 °C overnight. After evaporation, the residue was mixed with acetic acid (340 mL) and then evaporated at 45 °C in vacuo to remove traces of hydrochloric acid, followed by the same procedure using a 1:1 mixture of acetonitrile and toluene (780 mL) which was repeated until no HCl traces could be detected after evaporation (control with wet pH paper above the residue). The residue was recrystallized from acetonitrile to give the desired product as an off-white solid (9.8 g, 50% yield): ^{1}H NMR (500 MHz, DMSO-d_6) δ ppm 1.64−1.79 (m, 1 H), 1.87−2.00 (m, 1 H), 2.02−2.28 (m, 2 H), 2.66−2.79 (m, 1 H), 4.81−5.11 (m, 1 H). CO_2H and PO_3H_2 protons form a very broad peak between approximately 9 and 13 ppm. ^{19}F NMR (376 MHz, DMSO-d_6) δ ppm −191.5 (mc, 1 F, diastereomer 1), −189.2 (mc, 1 F, diastereomer 2). MS (ESI): $[M - H]^-$ = 243.

(2*S*,4*S*)-2-Fluoro-4-(phosphonomethyl)pentanedioic Acid ((2*S*,4*S*)-21). A mixture of (2*S*,4*S*)-**24** (3.83 g, 8.47 mmol) and 6 M hydrochloric acid (42 mL) was stirred at 50 °C for 12 h and then evaporated (to remove methanol formed by hydrolysis). Another portion of 6 M hydrochloric acid (42 mL) was added, and the mixture was stirred at 50 °C overnight. The mixture was again evaporated and then further processed, analogous to the procedure described for **21**, by addition of acetic acid followed by evaporation and subsequent repetition of the addition/evaporation procedure with an acetonitrile/toluene mixture until no HCl traces could be detected after evaporation (control with wet pH paper above the residue). Recrystallization from acetonitrile gave the crystalline product (1.77 g, 82% yield): ^{1}H NMR (400 MHz, DMSO-d_6) δ ppm 1.73 (ddd, J = 17.5, 15.2, 6.8 Hz, 1 H), 1.92 (ddd, J = 18.3, 15.2, 6.8 Hz, 1 H), 2.00−2.29 (m, 2 H), 2.63−2.77 (m, 1 H), 5.02 (ddd, J = 49.3, 9.0, 3.8 Hz, 1 H); ^{19}F NMR (376 MHz, DMSO-d_6) δ ppm −188.9. MS (ESI): $[M + H]^+$ = 245.

(2*S*,4*R*)-2-Fluoro-4-(phosphonomethyl)pentanedioic Acid (2*S*,4*R*)-21). A mixture of (2*R*,4*S*)-**24** (5.28 g, 11.7 mmol) and 6 M hydrochloric acid (58 mL) was stirred at 50 °C for 12 h and then evaporated (to remove methanol formed by hydrolysis). Another portion of 6 M hydrochloric acid (55 mL) was added, and the mixture was stirred at 50 °C overnight. The mixture was again evaporated and then further processed, analogous to the procedure described for **21**, by addition of acetic acid followed by evaporation and subsequent repetition of the addition/evaporation procedure with an acetonitrile/toluene mixture until no HCl traces could be detected after evaporation (control with wet pH paper above the residue). Recrystallization from acetonitrile gave the crystalline product (2.52 g, 84% yield): ^{1}H NMR (400 MHz, DMSO-d_6) δ ppm 1.69 (ddd, J =

dx.doi.org/10.1021/jm300710j | J. Med. Chem. XXXX, XXX, XXX−XXX

17.2, 15.4, 8.1 Hz, 1 H), 1.87−2.28 (m, 3 H), 2.65−2.80 (m, 1 H), 4.90 (ddd, J = 50.0, 10.4, 2.8 Hz, 1 H).

(2*R*,4*S*)-2-Fluoro-4-(phosphonomethyl)pentanedioic Acid (2*R*,4*S*)-21). A mixture of (2*S*,4*R*)-**24** (5.05 g, 11.2 mmol) and 6 M hydrochloric acid (55 mL) was stirred at 50 °C for 15 h and then evaporated (to remove methanol formed by hydrolysis). Another portion of 6 M hydrochloric acid (55 mL) was added, and the mixture was stirred at 50 °C overnight. The mixture was again evaporated and then further processed, analogous to the procedure described for **21**, by addition of acetic acid followed by evaporation and subsequent repetition of the addition/evaporation procedure with an acetonitrile/toluene mixture until no HCl traces could be detected after evaporation (control with wet pH paper above the residue). Recrystallization from acetonitrile gave the crystalline product (2.43 g, 85% yield): ^{1}H NMR (400 MHz, DMSO-d_6) δ ppm 1.69 (ddd, J = 17.2, 15.4, 8.1 Hz, 1 H), 1.87−2.28 (m, 3 H), 2.65−2.80 (m, 1 H), 4.90 (ddd, J = 50.0, 10.4, 2.8 Hz, 1 H); ^{19}F NMR (376 MHz, DMSO-d_6) δ ppm −191.1. MS (ESI): $[M + H]^+$ = 245.

(2*R*,4*R*)-2-Fluoro-4-(phosphonomethyl)pentanedioic Acid (2*R*,4*R*)-21). To a solution of (2*R*,4*R*)-**24** (340 mg, 752 μmol) in THF (6.5 mL) was added 6 M aqueous hydrochloric acid (6.5 mL), and the mixture was stirred at 100 °C for 1.5 h in a microwave oven. The mixture was evaporated and analyzed by ^{1}H NMR. To drive the reaction to completion, the residue was treated with 6 M aqueous hydrochloric acid (6.5 mL) and the mixture stirred again at 100 °C for 1.5 h. All volatiles were evaporated and the residue was purified by preparative reversed-phase HPLC to give the target compound (158 mg) which solidified upon standing. An aliquot (20 mg) was subjected to crystallization from MTBE/THF/hexane/toluene to give crystals suitable for X-ray analysis: ^{1}H NMR (600 MHz, DMSO-d_6) δ ppm 1.69−1.79 (m, 1 H), 1.87−1.96 (m, 1 H), 2.02−2.12 (m, 1 H), 2.14−2.25 (m, 1 H), 2.66−2.75 (m, 1 H), 5.01 (ddd, 1 H). MS (ESI): $[M + H]^+$ = 245. The crystals were subjected to X-ray analysis, revealing their (2*R*,4*R*) absolute configuration (Figure 8).

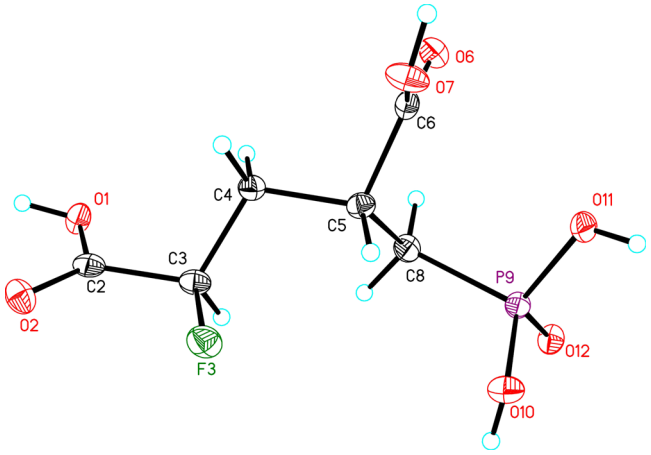

Figure 8. Empirical formula: $C_6H_{10}F_1O_7P_1$. Formula weight: 244.11g/mol. Temperature: 100(2) K. Wavelength: 1.541 78 Å. Crystal system: monoclinic. Space group: $P21$. Unit cell dimensions: a = 8.9000(12) Å, b = 5.3584(8) Å, c = 9.8181(14) Å, β = 91.273(7)°. Z = 2. Goodness-of-fit on F^2: 1.064. Final R indices $[I > 2\sigma(I)]$: R1 = 0.0227, wR2 = 0.0571. R indices (all data): R1 = 0.0231, wR2 = 0.0574. Absolute structure parameter: 0.043(19). The crystal structure has been deposited into the Cambridge Structural Database (CCDC 895587).

The preparation was scaled in analogy to the protocol described for the three preceding stereoisomers of **21** to give 0.93 g (78% yield) of (2*R*,4*R*)-**21** from (2*R*,4*R*)-**24** (2.10 g, 4.64 mmol): ^{1}H NMR (400 MHz, DMSO-d_6) δ ppm 1.73 (ddd, J = 17.5, 15.2, 6.8 Hz, 1 H), 1.92 (ddd, J = 18.3, 15.2, 6.8 Hz, 1 H), 2.00−2.29 (m, 2 H), 2.63−2.77 (m, 1 H), 5.02 (ddd, J = 49.3, 9.0, 3.8 Hz, 1 H).

Dimethyl (2*S*,4*S*)-2-Fluoro-4-(phosphonomethyl)-pentanedioate ((2*S*,4*S*)-25). To a solution of (2*S*,4*S*)-**24** (310 mg, 686 μmol) in THF (5 mL) was added a 10% palladium on charcoal catalyst (50 mg), and the resulting mixture was stirred at room temperature under an atmosphere of hydrogen for 2 h. The catalyst was filtered off over a plug of Celite, washed with acetonitrile, and all volatiles were removed in vacuo. The residue was analyzed by ^{1}H NMR, dissolved in dichloromethane (10 mL), and the mixture was cooled to −20 °C for 4 days, whereupon 130 mg (70% yield) of the crystalline product could be obtained. A fraction of the crystalline product was redissolved in dichloromethane and was allowed to concentrate slowly at −20 °C to give crystals suitable for X-ray analysis: ^{1}H NMR (300 MHz, DMSO-d_6) δ ppm 1.67−1.96 (m, 2 H), 2.01−2.36 (m, 2 H), 2.70−2.88 (m, 1 H), 3.57 (s, 3 H), 3.69 (s, 3 H), 5.21 (ddd, 1 H); no isomeric contamination could be detected as judged by comparison with the respective isomeric mixture prepared from **24** as described above. MS (ESI): $[M + H]^+$ = 273. The crystals were subjected to X-ray analysis revealing their (2*S*,4*S*) absolute configuration (Figure 9).

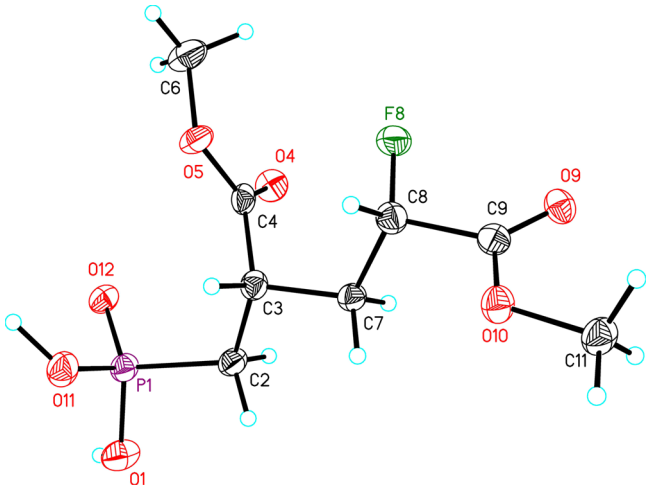

Figure 9. Empirical formula: $C_8H_{14}FO_7P$. Formula weight: 272.16 g/mol. Temperature: 100(2) K. Wavelength: 1.541 78 Å. Crystal system: monoclinic. Space group: $P21$. Unit cell dimensions: a = 6.135(4) Å, b = 6.066(5) Å, c = 15.731(4) Å, β = 94.04(3)°. Z = 2. Goodness-of-fit on F^2: 1.086. Final R indices $[I > 2\sigma(I)]$: R1 = 0.0232, wR2 = 0.0614. R indices (all data): R1 = 0.0234, wR2 = 0.0615. Absolute structure parameter: 0.04(2). The crystal structure has been deposited into the Cambridge Structural Database (CCDC 895588).

Dimethyl (*RS*)-2-{[*tert*-Butyl(dimethyl)silyl]oxy}-4-methylenepentanedioate (26). To a cooled (0 °C) solution of the starting alcohol **22** (2.00 g, 10.6 mmol) in dichloromethane (50 mL) was added *N*-methylimidazole (1.40 equiv), followed by *tert*-butyldimethylchlorosilane (TBS chloride, 1.30 equiv). The cooling bath was removed, and the mixture was allowed to stir overnight at room temperature. Subsequently, the double volume of dichloromethane was added and the solution was washed with brine twice. The organic layer was dried over sodium sulfate and evaporated. The residue was purified by column chromatography on silica to give 2.69 g of the target compound (84% yield): ^{1}H NMR (300 MHz, $CDCl_3$) δ ppm 0.00 (s, 3 H), 0.04 (s, 3 H), 0.87 (s, 9 H), 2.59 (dd, 1 H), 2.83 (dd, 1 H), 3.72 (s, 3 H), 3.76 (s, 3 H), 4.43 (dd, 1 H), 5.67 (m, 1 H), 6.26 (m, 1 H). MS (EI): $[M + H]^+$ = 303.

Dimethyl *rac*-2-{[Bis(benzyloxy)phosphoryl]methyl}-4-{[*tert*-butyl(dimethyl)silyl]oxy}pentanedioate (27). A mixture of **26** (1.88 g, 6.22 mmol), dibenzyl phosphite (1.72 mL, 1.25 equiv), and finely powdered potassium carbonate (1.29 g, 1.50 equiv) in DMF (40 mL) was heated to 90 °C for 2 h and was then allowed to stir at room temperature for 60 h. The mixture was then evaporated and partitioned between EtOAc and 5% aqueous citric acid. The organic layer was washed with half-concentrated brine, dried over sodium sulfate, and evaporated. The residue was purified by column

dx.doi.org/10.1021/jm300710j | J. Med. Chem. XXXX, XXX, XXX−XXX

chromatography over silica to give the desired product (3.43 g, 98% yield) as an oil: ^{1}H NMR (300 MHz, $CDCl_3$) δ ppm −0.02 to 0.08 (m, 6 H), 0.88 (s, 9 H, major diastereomer), 0.89 (s, 9 H, minor diastereomer), 1.84−2.35 (m, 4 H), 2.86−3.12 (m, 1 H), 3.53 (s, 3 H, major diastereomer), 3.55 (m, 3 H, minor diastereomer), 3.67 (m, 3 H, major diastereomer), 3.68 (m, 3 H, minor diastereomer), 4.14−4.24 (m, 1 H), 4.90−5.07 (m, 4 H), 7.28−7.40 (m, 10 H).

Dimethyl *rac*-2-{[Bis(benzyloxy)phosphoryl]methyl}-4-(tosyloxy)pentanedioate (28). To an ice-cooled solution of **27** (2.50 g, 4.43 mmol) in THF (100 mL) was added hydrogen fluoride−pyridine complex (5.75 mL, 50 equiv) under ice cooling, and the mixture was then stirred at room temperature for 4 h. Subsequently, a solution prepared from potassium hydroxide (18 g), boric acid (39.5 g), and water (180 mL) was carefully added until the pH reached 7. The mixture was carefully concentrated to largely remove THF, partitioned between water and MTBE, and the organic layer was washed with brine, dried over sodium sulfate, and evaporated. The residual crude γ-hydroxy ester (2.21 g) was immediately dissolved in pyridine (50 mL). *p*-Toluenesulfonic anhydride (3.19 g, 2.00 equiv based on crude hydroxy ester) was added, and the mixture was stirred for 16 h at room temperature. The mixture was then partitioned between water and MTBE, and the organic layer was washed with 5% aqueous citric acid and with brine, dried over sodium sulfate, and evaporated. The residue was purified by column chromatography to give the target compound as an oily mixture of stereoisomers (1.89 g, 70% overall yield): ^{1}H NMR (400 MHz, $CDCl_3$) δ ppm 1.83−2.07 (m, 1 H), 2.10−2.33 (m, 3 H), 2.43 (s, 3 H), 2.81−2.98 (m, 1 H), 3.51 (s, 3 H, minor diastereomer), 3.53 (s, 3 H, major diastereomer), 3.57 (s, 3 H, major diastereomer), 3.62 (s, 3 H, minor diastereomer), 4.88−5.05 (m 5 H), 7.28−7.41 (m, 12 H), 7.75−7.81 (m, 2 H). MS (ESI): $[M + H]^+$ = 605.

Dimethyl (*RS*)-2-Methylene-4-(tosyloxy)pentanedionate (29). To a cooled (0 °C) solution of the starting alcohol **22** (1.00 g, 5.31 mmol) in pyridine (20 mL) was added *p*-toluenesulfonic anhydride (3.47 g, 2.00 equiv), and the mixture was stirred for a period ranging from 2 h at 0 °C to 16 h at room temperature. The reaction mixture was then partitioned between water and dichloromethane. The organic layer was then washed with water and brine, dried over sodium sulfate, and evaporated. The crude product (1.80 g, 99% yield) was used without further purification: ^{1}H NMR (400 MHz, $CDCl_3$): δ ppm 2.45 (s, 3 H), 2.69 (dd, 1 H), 2.90 (dd, 1 H), 3.67 (s, 3 H), 3.68 (s, 3 H), 5.06 (dd, 1 H), 5.67 (s, 1 H), 6.21 (s, 1 H), 7.32 (d, 2 H), 7.75 (d, 2 H). MS (ESI): $[M + H]^+$ = 343.

Dimethyl *rac*-2-{[Bis(benzyloxy)phosphoryl]methyl}-4-(tosyloxy)pentanedioate (28, Optimized Preparation). To a solution of **26** (1.32 g, 3.81 mmol) in THF (40 mL) were added DBU (1,8-diazabicyclo(5.4.0)undec-7-ene, 717 μL, 1.25 equiv) and dibenzyl phosphite (1.70 mL, 2.00 equiv), and the mixture was stirred at room temperature for 1.5 h. The mixture was concentrated in vacuo and then partitioned between EtOAc and 5% aqueous citric acid. The organic layer was washed with brine, dried over sodium sulfate, and evaporated. The residue was purified by column chromatography on silica (hexane/EtOAc) to give the desired product (1.42 g, 61% yield) as a mixture of stereoisomers: ^{1}H NMR (400 MHz, $CDCl_3$) δ ppm 1.83−2.07 (m, 1 H), 2.10−2.33 (m, 3 H), 2.43 (s, 3 H), 2.81−2.98 (m, 1 H), 3.51 (s, 3 H, minor diastereomer), 3.53 (s, 3 H, major diastereomer), 3.57 (s, 3 H, major diastereomer), 3.62 (s, 3 H, minor diastereomer), 4.88−5.05 (m 5 H), 7.28−7.41 (m, 12 H), 7.75−7.81 (m, 2 H). MS (ESI): $[M + H]^+$ = 605.

***rac*-2-[^{18}F]Fluoro-4-(phosphonomethyl)pentanedioic Acid ([^{18}F]21).** [^{18}F]Fluoride (4.2 GBq) was immobilized on a preconditioned QMA (Waters) cartridge (preconditioned by washing the cartridge with 5 mL of 0.5 M potassium carbonate and 10 mL of water), The [^{18}F]fluoride was eluted using a solution of cesium carbonate (2.3 mg) in 500 μL of water and Kryptofix 2.2.2. (5 mg) in 1500 μL of acetonitrile. This solution was dried at 120 °C with stirring under vacuum, with a stream of nitrogen. Additional acetonitrile (1 mL) was added, and the drying step was repeated. A solution of precursor **27** (4 mg) in DMSO (500 μL) was added and heated at 120 °C for 15 min. The mixture was diluted with 15 mL of water and passed through a C18 light SPE (preconditioned with 5 mL of ethanol and with 10 mL of water). The C18 light SPE was washed with 5 mL of water and eluted with 1 mL of MeCN. The eluted solution was diluted with 3 mL of water and purified over preparative HPLC (ACE 5 μm C18, 250 mm × 10 mm, isocratic 60% MeCN in 40% water + 0.1% TFA, flow of 4 mL/min). The product peak was collected and diluted with 20 mL of water and passed through a C18 light SPE (preconditioned with 5 mL of ethanol and with 10 mL of water). The SPE was washed with 5 mL of water and was eluted with 1 mL of acetonitrile. The acetonitrile solution was dried under gentle N_2 stream for 10 min at 100 °C. An amount of 500 μL of 6 M HCl was added, and the mixture was incubated for 15 min at 120 °C. After cooling, the reaction mixture was diluted with 1 mL of water and passed through a cartridge containing AG11A8 resin (ion retardation resin, ∼11g) connected in series with a C18 light SPE (preconditioned with 5 mL of ethanol and with 10 mL of water). The cartridges were then washed with saline (5 mL) and eluents were collected to give the desired product [^{18}F]**21** (509 MBq, 29% d.c.) with a specific activity of >25GBq/μmol with a radiochemical purity of >95% as determined by HPLC with the ZIC-HILIC column and by TLC (silica, 1-butanol/acetic acid/water/ethanol (12:3:5:1.5)). The final preparation was always found to contain 3−4% free [^{18}F]fluoride.

NAALADase Assay. NAALAdase activity was assayed essentially as described previously.[38] Briefly, crude membrane extracts from LNCaP tissue culture cells (obtained from ATCC) were prepared by homogenization of the cells in lysis buffer (50 mM Tris-HCl, 150 mM NaCl, pH 7.4, glass Teflon potter, 300 rpm), separation of the nuclear fraction (1000*g*, 10 min), precipitation of the membrane fraction (100000*g*, 20 min), and resuspension in solubilization buffer (lysis buffer plus 1% Triton X-100). After a final centrifugation step (100000*g*, 20 min) the supernatant containing solubilized membrane proteins was frozen in liquid nitrogen and stored at −80 °C. Release of [^{3}H]glutamate from [^{3}H]-*N*-acetylaspartylglutamate (NAAG, assay concentration of 0.5 μM) in 50 mM Tris-HCl buffer, pH 7.4, after 30 min at 37 °C was measured using 2 μg/mL solubilized membrane protein. The enzymatic reaction was stopped by adding cold methanol. Substrate and product were resolved by cation-exchange liquid chromatography. Prefilled AG 50W-X8 columns (200−400 mesh, (BIO RAD, Hercules, CA) were equilibrated in 0.2 M HCl before loading with the enzymatic mixture. After a wash with 9 mL of 0.2 M HCl, fractions containing [^{3}H]glutamate were eluted with 6 mL of 2 M HCl, mixed with liquid scintillation fluid, and analyzed in a liquid scintillation analyzer. Under these assay conditions less than 20% of substrate was cleaved. Inhibition curves were generated by semi-logarithmic plotting of enzyme activity versus inhibitor concentration and IC_{50} values determined by curve fitting using the software GraFit5 (version 5.0.6). Reported values represent the mean and standard deviation of two to four replicates of the entire inhibition study. K_i values were calculated according to the method of Cheng and Prusoff.[39]

In Vivo Animal Studies. All animal experiments were performed in compliance with the current version of the German law concerning animal protection and welfare. PET imaging studies with tumor bearing nude mice were performed using the Inveon small animal PET/CT scanner (Siemens, Knoxville, TN). Male Balb/c nude mice (n = 5; Charles-River, Sulzfeld, Germany) were used for subcutaneous inoculation of human xenografts. At 3−4 days before injection of tumors cells, a testosterone pellet (Innovative Research of America, catalog no. NA-151) was implanted. LNCaP (human prostate cancer) tumor cells (1 × 10^7 cells per animal in 100 μL of Matrigel) were injected subcutaneously into the right flank and allowed to grow for approximately 4 weeks, reaching sizes of 5−8 mm in diameter. Animals (n = 4) were injected intravenously with 10 MBq compound [^{18}F]**21**. Immediately prior to imaging, the animals were anesthetized with isoflurane, and the PET data were acquired over defined time periods after injection.

dx.doi.org/10.1021/jm300710j | *J. Med. Chem.* XXXX, XXX, XXX−XXX

AUTHOR INFORMATION

Corresponding Author

*Phone: +49 (0) 468 192114. Fax: (+) 49 (0) 468 992114. E-mail: keith.graham@bayer.com.

Notes

The authors declare the following competing financial interest(s): All the authors are employees of Bayer Healthcare.

ACKNOWLEDGMENTS

The authors acknowledge the excellent technical assistance of Selahattin Ede, Mario Mandau, Marion Zerna, Rene Zernicke, Jörg Jannsen, Eva-Maria Bickel, Uwe Rettig, Yvonne Duchstein, Oliver Schenk, and Anika Hans.

ABBREVIATIONS USED

CAD, Corona aerosol detection; DBU, 1,8-diazabicycloundec-7-ene; DMF, dimethylformamide; DMSO, dimethyl sulfoxide; EtOAc, ethyl acetate; HPLC, high pressure liquid chromatography; MTBE, methyl *tert*-butyl ether; NAAG, *N*-acetylaspartylglutamate; NAALADase, N-acetylated α linked acidic dipeptidase; nca, no-carrier-added; NMR, nuclear magnetic resonance; PET, positron emission tomography; PTC, phase transfer catalyst; 2-PMPA, 2-(phosphonomethyl)pentanedioic acid; PSA, prostate specific antigen; PSMA, prostate specific membrane antigen; SPECT, single photon emission computed tomography; SPE, solid phase extraction; TBAF, tetrabutylammonium fluoride; THF, tetrahydrofuran

REFERENCES

(1) Jemal, A; Siegel, R; Xu, J; Ward, E. Cancer Statistics, 2010. *Ca—Cancer J. Clin.* **2010**, *60* (Sep−Oct), 277−300.

(2) Tasch, J.; Gong, M.; Sadelain, M.; Heston, W. D. A unique folate hydrolase, prostate-specific membrane antigen (PSMA): a target for immunotherapy. *Crit. Rev. Immunol.* **2001**, *21*, 249−261.

(3) Schulke, N.; Varlamova, O. A.; Donovan, G. P.; Ma, D.; Gardner, J. P.; Morrissey, D. M.; Arrigale, R. R.; Zhan, C.; Chodera, A. J.; Surowitz, K. G.; Maddon, P. J.; Heston, W. D.; Olson, W. C. The homodimer of prostate-specific membrane antigen is a functional target for cancer therapy. *Proc. Natl. Acad. Sci. U.S.A.* **2003**, *100*, 12590−12595.

(4) Chang, S. S.; Reuter, V. E.; Heston, W. D.; Bander, N. H.; Grauer, L. S.; Gaudin, P. B. Five different anti-prostate-specific membrane antigen (PSMA) antibodies confirm PSMA expression in tumor associated neovasculature. *Cancer Res.* **1999**, *59*, 3192−3198.

(5) Lapidus, R. G.; Tiffany, C. W.; Isaacs, J. T.; Slusher, B. S. Prostate specific membrane antigen (PSMA) enzyme activity is elevated in prostate cancer cells. *Prostate* **2000**, *45*, 350−354.

(6) Scher, B.; Seitz, M.; Albinger, W.; Tiling, R.; Scherr, M.; Becker, H. C.; Souvatzogluou, M.; Gildehaus, F. J.; Wester, H. J.; Dresel, S. Value of ^{11}C-choline PET and PET/CT in patients with suspected prostate cancer. *Eur. J. Nucl. Med. Mol. Imaging* **2007**, *34*, 45−53.

(7) Rinnab, L.; Mottaghy, F. M.; Blumstein, N. M.; Reske, S. N.; Hautmann, R. E.; Hohl, K.; Moller, P.; Wiegel, T.; Kuefer, R.; Gschwend, J. E. Evaluation of [^{11}C]-choline positron-emission/computed tomography in patients with increasing prostate-specific antigen levels after primary treatment for prostate cancer. *BJU Int.* **2007**, *100*, 786−793.

(8) Reske, S. N.; Blumstein, N. M.; Neumaier, B.; Gottfried, H. W.; Finsterbusch, F.; Kocot, D.; Moller, P.; Glatting, G.; Perner, S. Imaging prostate cancer with ^{11}C-choline PET/CT. *J. Nucl. Med.* **2006**, *47*, 1249−1254.

(9) Zophel, K.; Kotzerke, J. Is ^{11}C-choline the most appropriate tracer for prostate cancer? Against. *Eur. J. Nucl. Med. Mol. Imaging* **2004**, *31*, 756−759.

(10) Vees, H.; Buchegger, F.; Albrecht, S.; Khan, H.; Husarik, D.; Zaidi, H.; Soloviev, D.; Hany, T. F.; Miralbell, R. ^{18}F-choline and/or ^{11}C-acetate positron emission tomography: detection of residual or progressive subclinical disease at very low prostate-specific antigen values (<1 ng/mL) after radical prostatectomy. *BJU Int.* **2007**, *99*, 1415−1420.

(11) Schuster, D. M.; Votaw, J. R.; Nieh, P. T.; Yu, W.; Nye, J. A.; Master, V.; Bowman, F. D.; Issa, M. M.; Goodman, M. M. Initial experience with the radiotracer anti-1-amino-3-^{18}F-fluorocyclobutane-1-carboxylic acid with PET/CT in prostate carcinoma. *J. Nucl. Med.* **2007**, *48*, 56−63.

(12) Larson, S. M.; Morris, M.; Gunther, I.; Beattie, B.; Humm, J. L.; Akhurst, T. A.; Finn, R. D.; Erdi, Y.; Pentlow, K.; Dyke, J.; Squire, O.; Bornmann, W.; McCarthy, T.; Welch, M.; Scher, H. Tumor localization of 16beta-^{18}F-fluoro-5alpha-dihydrotestosterone versus ^{18}F-FDG in patients with progressive, metastatic prostate cancer. *J. Nucl. Med.* **2004**, *45*, 366−373.

(13) Tehrani, O. S.; Muzik, O.; Heilbrun, L. K.; Douglas, K. A.; Lawhorn-Crews, J. M.; Sun, H.; Mangner, T. J.; Shields, A. F. Tumor imaging using 1-(2′-deoxy-2′-^{18}F-fluoro-beta-D-arabinofuranosyl)-thymine and PET. *J. Nucl. Med.* **2007**, *48*, 1436−1441.

(14) Byun, Y; Mease, R. C.; Lupold, S; Pomper, M. G. Recent Development of Diagnostic and Therapeutic Agents Targeting Glutamate Carboxypeptidase II (GCPII). In *Drug Design of Zinc-Enzyme Inhibitors*; Superan, C. T., Winum, J.-Y., Eds.; Wiley: Hoboken, NJ, 2009.

(15) Tsukamoto, T; Wozniak, K. M.; Slusher, B. S. Progress in the discovery and development of glutamate carboxypeptidase II inhibitors. *Drug Discovery Today* **2007**, *12*, 767−776.

(16) Foss, C. A.; Mease, R. C.; Fan, H.; Wang, Y.; Ravert, H. T.; Dannals, R. F.; Olszewski, R.; Heston, W. D.; Kozikowski, A. P.; Pomper, M. G. Radiolabeled small molecule ligands for prostate-specific membrane antigen: in vivo imaging in experimental models of prostate cancer. *Clin. Cancer Res.* **2005**, *11*, 4022−402.

(17) Mease, R. C.; Dusich, C. L; Foss, C. A; Ravert, H. T.; Dannals, R. F.; Seidel, J.; Prideaux, A.; Fox, J. J.; Sgouros, G.; Kozikowski, A. P.; Pomper, M. G. *N*-[*N*-[(*S*)-1,3-Dicarboxypropyl]carbamoyl]-4-[^{18}F]-fluorobenzyl-L-cysteine, [^{18}F]DCFBC: a new imaging probe for prostate cancer. *Clin. Cancer Res.* **2008**, *14* (10), 3036−3043.

(18) Maresca, K. P.; Hillier, S. M.; Fernia, F. J.; Keith, D.; Barone, C.; Joyal, J. L.; Zimmerman, C. N.; Kozikowski, A. P.; Barrett, J. A.; Eckelman, W. C.; Babich, J. W. A series of halogenated heterodimeric inhibitors of prostate specific membrane antigen (PSMA) as radiolabeled probes for targeting prostate cancer. *J. Med. Chem.* **2009**, *52* (2), 347−357.

(19) Chen, Y.; Foss, C. A.; Byun, Y.; Nimmagadda, S.; Pullambhatla, M.; Fox, J. J.; Castanares, M.; Lupold, S. E.; Babich, J. W.; Mease, R. C.; Pomper, M. G. Radiohalogenated prostate-specific membrane antigen (PSMA)-based ureas as imaging agents for prostate cancer. *J. Med. Chem.* **2008**, *51* (24), 7933−7943.

(20) Banerjee, S. R.; Pullambhatla, M.; Byun, Y.; Nimmagadda, S.; Green, G.; Fox, J. J.; Horti, A.; Mease, R. C.; Pomper, M. G. ^{68}Ga-Labeled inhibitors of prostate-specific membrane antigen (PSMA) for imaging prostate cancer. *J. Med. Chem.* **2010**, *53* (14), 5333−5341.

(21) Lapi, S. E.; Wahnishe, H.; Pham, D.; Wu, L. Y.; Nedrow-Byers, J. R.; Liu, T.; Vejdani, K.; VanBrocklin, H. F.; Berkman, C. E.; Jones, E. F. Assessment of an ^{18}F-labeled phosphoramidate peptidomimetic as a new prostate-specific membrane antigen-targeted imaging agent for prostate cancer. *J. Nucl. Med.* **2009**, *50* (12), 2042−2048.

(22) Misra, P.; Humblet, V.; Pannier, N.; Maison, W.; Frangioni, J. V. Production of multimeric prostate-specific membrane antigen small-molecule radiotracers using a solid-phase ^{99m}Tc preloading strategy. *J. Nucl. Med.* **2007**, *48* (8), 1379−1389.

(23) Banerjee, S. R.; Foss, C. A.; Castanares, M.; Mease, R. C.; Byun, Y.; Fox, J. J.; Hilton, J.; Lupold, S. E.; Kozikowski, A. P.; Pomper, M. G. Synthesis and evaluation of technetium-99m- and rhenium-labeled inhibitors of the prostate-specific membrane antigen (PSMA). *J. Med. Chem.* **2008**, *51* (15), 4504−4517.

(24) Vitharana, D.; France, J. E.; Scarpetti, D.; Bonneville, G. W.; Majer, P.; Tsukamoto, T. Synthesis and biological evaluation of (*R*)- and (*S*)-2-(phosphonomethyl)pentanedioic acids as inhibitors of glutamate carboxypeptidase II. *Tetrahedron: Asymmetry* **2002**, *13*, 1609−1614.
(25) Jackson, P. F.; Cole, D. C.; Slusher, B. S.; Stetz, S. L.; Ross, L. E.; Donzanti, B. A.; Trainor, D. A. Design, synthesis, and biological activity of a potent inhibitor of the neuropeptidase N-acetylated α-linked acidic dipeptidase. *J. Med. Chem.* **1996**, *39* (15), 619−622.
(26) Kozikowski, A. P.; Zhang, J.; Nan, F.; Petukhov, P. A.; Grajkowska, E.; Wroblewski, J. T.; Yamamoto, T.; Bzdega, T.; Wroblewska, B.; Neale, J. H. Synthesis of urea-based inhibitors as active site probes of glutamate carboxypeptidase II: efficacy as analgesic agents. *J. Med. Chem.* **2004**, *47* (7), 1729−1738.
(27) Wang, H.; Byun, Y.; Barinka, C.; Pullambhatla, M.; Bhang, H. C.; Fox, J. J.; Lubkowski, J.; Mease, R. C.; Pomper, M. G. Bioisosterism of urea-based GCPII inhibitors: synthesis and structure−activity relationship studies. *Bioorg. Med. Chem. Lett.* **2010**, *20*, 392−397.
(28) For reviews see the following: (a) Vorbrüggen, H. *Helv. Chim. Acta* **2011**, *94*, 947−965. (b) Takamatsu, S.; Katayama, S.; Hirose, N.; De Cock, E.; Schelkens, G.; Demillequand, M.; Brepoels, J.; Isawa, K. *Nucleotsides, Nucleotides Nucleic Acids* **2002**, *21*, 849−861.
(29) For a more extended discussion of stereochemical assignments see the following: Graham, K.; Kettschau, G.; Lesche, R.; Gromov, A.; Böhnke, N.; Hassfeld, J. WO 2011/073286, 2011.
(30) Paschlau, J. Schwerpunkt chromatographie—Corona CAD—eine neue detektionsmethode fur die HPLC. *GIT Labor-Fachz.* **2005**, *49*, 32−33.
(31) Gamache, P. H.; McCarthy, R. S.; Freeto, S. M.; Asa, D. J.; Woodcock, M. J.; Laws, K.; Cole, R. O. HPLC analysis of non-volatile analytes using charged aerosol detection. *LC-GC Eur.* **2005**, *18*, 345−354.
(32) Robinson, M. B.; Blakely, R. D.; Couto, R.; Coyle, J. T. Hydrolysis of the brain dipeptide *N*-acetyl-L-aspartyl-L-glutamate. *J. Biol. Chem.* **1987**, *262*, 14498−14506.
(33) Troyer, J. K.; Beckett, M. L.; Wright, G. L., Jr. Detection and characterization of the prostate specific membrane antigen (PSMA) in tissue extracts and body fluids. *Int. J. Cancer.* **1995**, *62*, 552−558.
(34) Silver, D. A.; Pellicer, I.; Fair, W. R.; Heston, W. D.; Cordon-Cardo, C. Prostate-specific membrane antigen expression in normal and malignant human tissues. *Clin. Cancer Res.* **1997**, *3*, 81−85.
(35) Slusher, B. S.; Tsai, G.; Yoo, G.; Coyle, J. T. Immunocytochemical localization of the *N*-acetyl-aspartyl-glutamate (NAAG) hydrolyzing enzyme N-acetylated alpha-linked acidic dipeptidase (NAALADase). *J. Comp. Neurol.* **1992**, *315*, 217−229.
(36) *PROTEUM2*, version 2009; Bruker, AXS Inc.: Madison, WI, U.S., 2009.
(37) Sheldrick, G. M. A short history of SHELX. *Acta Crystallogr.* **2008**, *A64*, 112−122.
(38) Fuhrman, S.; Palkovits, M.; Cassidy, M.; Neale, J. H. The regional distribution of *N*-acetylaspartylglutamate (NAAG) and peptidase activity against NAAG in the rat nervous system. *J. Neurochem.* **1994**, *62*, 275−281.
(39) Cheng, H. C. The power issue: determination of K_B or K_i from IC_{50}. A closer look at the Cheng−Prusoff equation, the Schild plot and related power equations. *J. Pharmacol. Toxicol. Methods* **2001**, *46*, 61−71.